

**KERNFORSCHUNGSZENTRUM
KARLSRUHE**

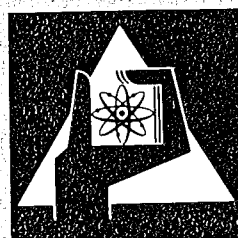
Juli 1974

KFK 2012

Institut für Angewandte Systemtechnik und Reaktorphysik
Projekt Schneller Brüter

Physics Investigations of Sodium Cooled Fast Reactors
SNEAK-Assembly 9B
Part 1

compiled by
G. Jourdan



**GESELLSCHAFT
FÜR
KERNFORSCHUNG M.B.H.**

KARLSRUHE

Als Manuskript vervielfältigt

Für diesen Bericht behalten wir uns alle Rechte vor

GESELLSCHAFT FÜR KERNFORSCHUNG M. B. H.
KARLSRUHE

KERNFORSCHUNGSZENTRUM KARLSRUHE

1974

KFK 2012

Institut für Angewandte Systemtechnik und Reaktorphysik
Projekt Schneller Brüter

Physics Investigations of Sodium Cooled Fast Reactors

SNEAK-Assembly 9B

Part 1

compiled by

G. Jourdan

With contributions from

E.A. Fischer, F. Helm, E. Korthaus, P.E. Mc Grath,
W.J. Oosterkamp, R. Papp, M. Pinter, A.M. Elbel-
Raberain, D. Wintzer, G. Wittek

Gesellschaft für Kernforschung mbH., Karlsruhe

Physikalische Untersuchungen an schnellen natriumgekühlten Reaktoren

SNEAK-Anordnung 9B

Teil 1

Zusammenfassung

Die Anordnung SNEAK-9 diente der physikalischen Untersuchung eines schnellen natriumgekühlten Brüter-Cores, das wesentliche Züge des Prototyps SNR trug. Infolge der verschiedenen Ziele war es notwendig, die Anordnung SNEAK-9 in drei verschiedenen Modifikationen aufzubauen: SNEAK-9A, SNEAK-9B und SNEAK-9C.

SNEAK-9B war ein Core mit drei Zonen; einer inneren Plutonium-Zone, einer Uranzone und der Blanketzone. In der Plutonium-Zone wurde ein sehr einfacher Zellaufbau gewählt, um die Auswertung der Experimente zu erleichtern. Wichtige Messungen in dieser Zone waren unter anderem: Natrium-void-Messungen von großen Zonen, Absorberwert- und Reaktionsratenmessungen.

Die experimentellen Ergebnisse wurden mit detaillierten Rechnungen verglichen.

Der Bericht besteht aus zwei Teilen. Im ersten Teil sind alle an SNEAK-9B durchgeführten Experimente außer den Reaktionsratenmessungen beschrieben. Die Beschreibung und Auswertung dieses fehlenden Experiments folgt im zweiten Teil.

Die in diesem Bericht beschriebenen Arbeiten wurden in enger Zusammenarbeit mit dem Industriekonsortium SNR und der französischen MASURCA-Gruppe in Cadarache durchgeführt.

Physics Investigations of Sodium Cooled Fast Reactors

SNEAK-Assembly 9B

Part 1

Abstract

SNEAK-Assembly 9 was aimed at measuring physics parameters of a fast sodium cooled breeder having a number of features typical for the prototype SNR. As a consequence of the different aims it was necessary to build the assembly SNEAK-9 in three modifications: SNEAK-9A, SNEAK-9B and SNEAK-9C.

SNEAK-9B has three zones, an inner Pu-zone, an uranium zone and the blanket zone. The cell of the Pu-zone was very simple to ease the evaluation of the experiments. Important measurements in this zone were: Sodium void measurements of large zones, absorber worth- and reaction rate measurements.

The experimental results were compared to detailed calculations.

The report consists of two parts. In the first part all experiments performed in SNEAK-9B are described except the reaction rate measurements. The reaction rate measurements and their evaluation are described in the second part.

The work covered by this report was performed in close cooperation with the industrial consortium for the SNR and the French MASURCA group at Cadarache.

19.6.1974

Table of Contents

	Page
1. Introduction	1
2. General description of the calculational methods	2
3. Description of the geometry and compositions	2
4. Critical experiment of SNEAK-9B	4
4.1 Experimental results	4
4.2 Methods and results of the k_{eff} calculations	4
5. Material worth determination	6
5.1 Description of the experiments	6
5.2 Description of the calculations	6
6. Buckling measurements	7
6.1 Description of the experiments	7
6.2 Methods and results of the B^2 evaluation	8

	Page
7. Comparison of absorber materials	9
7.1 Description of the experimental arrangement	9
7.2 Description of the calculational methods	10
7.2.1 Evaluation of the central measurements	10
7.2.2 Evaluation of the eccentric measurements	13
8. Sodium void measurements	13
8.1 Sodium void in axial direction	13
8.1.1 Description of the experiments	13
8.1.2 Description of the calculational methods	14
8.2 Sodium void effect of large sodium void zones	15
8.2.1 Description of the experiments	15
8.2.2 Description of the calculational methods	16
9. Doppler reactivity measurements	16
9.1 Description of the experiments	16
9.2 Comparison with calculations	17
Acknowledgements	19
References	20
Tables	23
Figures	37

1. Introduction

SNEAK-9B was one modification of the series of assemblies SNEAK-9, which were designed for investigating important physics parameters of a sodium cooled fast core of the SNR-type. Of particular interest in SNEAK-9B were reaction rate measurements in the core and blanket zones to calculate the breeding ratio. Other important measurements were large sodium void and absorber worth measurements.

Design and evaluation of the experiments were performed in close cooperation with the industrial consortium for the construction of the SNR and partially with French scientists of the fast critical facility MASURCA.

SNEAK-9B was a cylindrical core with two core zones. The central zone was fueled with plutonium. The outer zone was an uranium driver zone and then followed a blanket zone.

The experimental techniques applied in SNEAK-9B were already utilized during the SNEAK-2 and SNEAK-6 experiments. These are described in /1/ and /2/. The methods of evaluating the experiments are described in the chapter 2.

The experimental work on SNEAK-9 started with the assembly SNEAK-9B in the middle of January 1972. The work on SNEAK-9B was completed in the end of August 1972.

2. General description of the calculational methods

The SNEAK-9B evaluations were generally performed using the methods already used for SNEAK-6 and SNEAK-2 which were described in /1/ and /2/. These methods will not be described in detail here again.

The cross-section set used were the Karlsruhe 26-group sets MOXTOT /3/ and KFKINR /4/. The recently developed KFKINR-set was the basis set and the MOXTOT-set was employed additionally in order to simplify the comparison of results between SNEAK-6 and SNEAK-9B.

Diffusion theory was used in the whole series of calculations but some calculations used transport methods as a complement. The transport-codes used were the one-dimensional code DTK /9/ and the two-dimensional code SNOW /10/.

The heterogeneity-codes ZERA /5/ and KAPER /6/ were used, also, for some special investigations, the 208-group formalism /7/ and the REMO-method /8/.

3. Description of the geometry and the compositions

Assembly SNEAK-9B had two core zones. The height of the core was 90 cm.

Fig. 3 and 4 show a horizontal and a vertical section through the critical configuration, together with the critical dimensions which were used in the calculations.

The cell of the Pu-zone was chosen in such a way that:

- 1) The geometry should be very simple to ease the evaluation of the experiments.
- 2) The spectrum of this zone should be similar to that of the SNR central zone.

The outer core zone was an uranium driver zone.

The upper and lower axial blanket for both zones had a composition which simulated a breeder blanket of a power reactor. The radial blanket was depleted uranium.

The SNEAK-control rods of the inner zone were fueled with uranium, because only a few suitable Pu platelets are available. The positions of these rods were selected in such a way that the uranium filling would not perturb the experiments.

Fig. 1 shows the structure of the unit cells in each zone and the rest cells.

Fig. 2 shows the structure of the unit and rest cells of the SNEAK-control rods.

For deriving compositions to be used in k_{eff} -calculations the inner core zone was subdivided in two concentric parts.

The composition for the inner part takes into account only the unit cells and the rest cells used at the upper and lower core boundary. The composition of the outer part of the inner zone and that of the driver zone include the contributions of the SNEAK-control rods.

Both types of compositions are given for all zones in Table 1. The amount of gold (which was present in the soldering material of the Pu-platelets) was simulated in the calculations by B-10. A second type of composition which was used for the calculation of more local effects corresponds in each zone to the pure unit cells.

4. Critical experiment of SNEAK-9B

4.1 Experimental results

The measured k_{eff} value of the critical configuration of SNEAK-9B (as shown in Fig. 4, with all SNEAK-control rods in their most re-active position) was

$$k_{\text{eff}} = 1.0001 .$$

4.2 Methods and results of the k_{eff} calculations

The calculations for the critical experiment were performed with the usual methods, as described in /1/ and /2/. The basic calculation was a two-dimensional homogeneous diffusion calculation with 26-groups in R-Z-geometry. Fig. 4 shows the geometry and Table 1 the compositions utilized.

In the calculations the average mesh-size was 1 cm for the core zone and 2-3 cm in the blanket region. The numerical accuracy of the calculations was 1×10^{-4} in k_{eff} .

Some corrections were computed in one- or two-dimensional geometry and 26-groups.

- a) Heterogeneity correction
(influence of the platelet cell structure)

- b) REMO-correction
(improvement of the elastic removal cross-sections
in the first 14 energy groups)

- c) Transport correction
(S_6 -correction) - The transport correction was
calculated in two-dimensional
R-Z-geometry.

- d) The correction for cylindrization was found by
comparing a one-dimensional cylindrical diffu-
sion calculation with a two-dimensional diffu-
sion calculation in X-Y-geometry; both with the
same axial bucklings.

All calculations were performed with the KFKINR-set, most of them were repeated with the MOXTOT-set.

Table 6 gives the corrections and the final results for both cross-section sets. It appears that the MOXTOT-set calculated the experimental results very well, however, according to experience from other critical assemblies, this is due to a compensation of an

underestimate of the plutonium zone reactivity and an overestimate of the uranium driver zone. The KFKINR-set shows a slight overestimate ($\sim .6\%$).

5. Material worth determination

5.1 Description of the experiments

The material worth measurements in SNEAK-9B were performed with the pile oscillator. The worth of fuel isotopes, absorber- and structural materials were measured.

5.2 Description of the calculations

The calculated results were obtained using the following methods:

- 1) two-dimensional diffusion perturbation theory and homogeneous cross-sections with 26-groups in R-Z-geometry
- 2) a heterogeneity correction with the cell code KAPER, which takes into account the heterogeneity of the probe and the environment.

All the calculations were performed with the KFKINR-cross-section-set.

Table 7 gives the experimental and calculated results.

6. Buckling measurements

6.1 Description of the experiments

One method for a direct B_m^2 -determination is based on the measurement of reaction rate traverses. Traverses are measured with fission chambers of various fissile materials. In order to get an accurate value for the buckling from the curvature of these traverses the influence of the higher spectral modes induced by the blanket of the reactor must be eliminated. A method to separate the higher modes from the fundamental mode is described in /11/. But this procedure yields incorrect results if the inner zone of a reactor is so small, that throughout its volume the neutron spectrum is influenced considerably by the outer zone. Hence a modified method was developed /12/, which will be described here briefly.

From orthogonality it follows that a detector should have the cross-section proportional $D(E) \times \phi_0^+(E)$ to yield a traverse exactly proportional to the fundamental mode ($\phi_0^+(E)$ is the asymptotic adjoint flux). Since such a detector does not exist, one uses the following procedure:

Four traverses are measured with different fission chambers (^{235}U , ^{238}U , ^{237}Np , ^{239}Pu). These same traverses and the traverse of a fictitious detector with the cross-section $D(E)\phi_0^+(E)$ are calculated. Now a "semiexperimental $D\phi^+$ -traverse" is derived from the 4 measured and the 5 calculated traverses by applying a linear regression method to each point of measurements. Before the regression is performed, the measured values are smoothed by polynomial fits of the 8th order. Depending on the geometry, the material buckling is finally determined by a cosine or J_0 fit to the resultant semiexperimental $D\phi^+$ -traverse.

The fission chambers used for the experiment are only 6 mm in diameter and have an active length of 25 mm. The experimental channel can be quite small and results in a negligible perturbation. A comparison of traverses measured with chambers and foils did not show any systematic deviation in the region considered for the buckling measurement. Fine structure is largely smoothed by the length of the chambers. It becomes measurable only for the radial ^{238}U -traverses, where its influence must be eliminated by a suitable choice of the measuring positions.

Error calculations show that the error of B_m^2 due to counting statistics is small (about 0.1%). Somewhat larger systematic errors are due to the calculation of the traverses and to the linear regression. The attainable accuracy for B_m^2 is therefore probably in the vicinity of 0.3%.

6.2 Methods and results of the B^2 evaluation

The calculations were performed with a zero-dimensional program, iterating to a k_{eff} , which is equal 1.0 minus heterogeneity- and REMO-corrections. The MOXTOT- and KFKINR-cross-section-sets were used. Table 8 gives the experimental and calculated results.

One notes that the calculations overestimate the experimental results in both cases; but one has to note that in all assemblies in which bucklings are measured and evaluated the calculations overestimate the experimental results.

7. Comparison of absorber materials

In SNEAK-9B the effect of three types of absorber material was studied in the normal core spectrum and in a Na-voided zone. The purpose of these experiments was to test the usefulness of these materials as control rod materials.

7.1 Description of the experimental arrangement

The three absorber materials were tantalum (metallic), Eu_2O_3 and natural B_4C in powder form. For a better comparison for all absorbers the same geometrical arrangement was chosen. The metallic tantalum is in the form of rodlets and therefore the B_4C - and the Eu_2O_3 -powder was filled in aluminium tubes which were closed by welding. These rodlets (they had two different diameters) were placed in an aluminium-matrix. The absorber material and the aluminium-matrix together formed the absorber zone.

The absorber zone has a height of 12.1 cm and extended over four SNEAK-elements. Fig. 5 shows the cross-section of the absorber zone and Table 2 gives the compositions. For the measurements the absorber zone was located at the central and at an eccentric position in the normal core and then at the same positions in the voided core. In this core configuration the eccentric positions was at the boundary of largest void zone. Fig. 6 shows the positions of the measurements.

The central measurements in the normal core were performed in 4 steps. The reference core was the core with the aluminium-matrix.

1. step the reactivity of the four central small rodlets was measured

2. step four large rodlets were added

3. step four more large rodlets were added

4. step all the rodlets (8 small and 8 large ones) were in the matrix.

In the difference of the reactivity worth between step two and three one could study the mutual shadowing effect of the absorber material. In the void case and in the central position only the reactivity effect of step four was measured.

7.2 Description of the calculational methods

7.2.1 Evaluation of the central measurements

The calculations for the central experiment in the normal core and in the voided core are two-dimensional diffusion calculations in R-Z-geometry. The KFKINR-cross-section-set was used.

Fig. 7a shows the geometry model for the R-Z-calculations. The four central rodlets were homogenized with part of the surrounding aluminium of the matrix and the stainless steel of the core-tubes. The

eight large rodlets were simulated in a ring-model. The volume of the ring was nearly the same as the volume of the eight rodlets. For calculating step four of the measurements the entire absorber block (including aluminium and steel) was homogenized.

With these three models step number one, three and four of the central measurements were calculated.

In the case of step number two the absorber density in the ring was reduced by 50%.

In addition some corrections were calculated. These corrections were calculated only for B_4C but applied for all materials.

a) The influence of the exact geometry of the rodlets
in the matrix

This influence was calculated by comparison of one-dimensional radial calculations and two-dimensional X-Y-calculations with the same axial bucklings. These calculations were performed for each step of the measurements.

The geometry of the one-dimensional calculations corresponds also to the ring-model given in Fig. 7a. For the X-Y-calculations the rodlets were represented by polygons (see Fig. 7b). The effect was small in each step ($< -3\%$).

a) Transport correction

The transport correction was derived from one-dimensional radial S_8 -calculations for step number one, three and four of the measurements. The effect was small ($\sim -3\%$) for each step.

c) Heterogeneity effect of the surrounding material

The comparison of one-dimensional radial calculations with cross-sections of the homogenized core material and calculations with heterogeneity corrected cross-sections show the influence of the platelet-structure of the core material. The effect is very small ($\sim 1\%$).

Table 9a gives the experimental and the calculated results (with all corrections) of the central measurements in the normal core.

In the voided core only step number four (all absorber material in the aluminium matrix) was measured. The calculations for these measurements were performed in the same way as described above.

Table 9b gives the results of the experiments and the calculations.

7.2.2 Evaluation of the eccentric measurements

The calculations of the eccentric measurements in the normal core environment and in the voided core were performed using two-dimensional perturbation theory in R-Z-geometry. Table 9c gives the results of the eccentric measurements in the normal and in the voided core and the results of the calculations.

For all these values the reference core was the core with the Al-matrix (absorber holes filled by Al-plugs). Table 9d gives the experimental and calculated worth of the Al-matrix in all cases.

For comparison in the B_4C -case some calculations were performed with the MOXTOT-cross-section-set. One notes that this cross-section-set calculates the B_4C -values $\sim 6\%$ higher than the KFKINR-cross-section set.

8. Sodium void measurements

8.1 Sodium void in axial direction

8.1.1 Description of the experiments

The following measurements of the axial sodium void effect were performed in SNEAK-9B:

- 1) With the normal cell and in a way that was used in other SNEAK-assemblies. Fig. 8 gives the voided cells and Table 3 the composition.

- 2) With a slightly modified unit cell which allowed to orient the platelets both vertically and horizontally to the core-axis. This experiment was performed to study the influence of anisotropic diffusion. Fig. 9 gives the cell structure and Table 4 the cell averaged composition. Table 5 gives the compositions of the platelets used. These numbers were utilized in the heterogeneity calculations. In each case the void zones were enlarged stepwise in the four central elements from a small central void zone to the full core height.

8.1.2 Description of the calculational methods

The calculated results were obtained for the normal measurements and for the measurements of the anisotropic effect in different ways:

- 1) Axial sodium void with normal cells

Calculations were performed in general using perturbation theory in two dimensions and R-Z-geometry. The cross-section-sets used were the KFKINR-set and the MOXTOT-set. The cross-sections were heterogeneity corrected with the code ZERA. This renders possible a better comparison with results from SNEAK-2 and SNEAK-6. Fig. 10 shows the experimental and calculated results.

2) Axial sodium void with the modified cells

The calculations were performed using one-dimensional perturbation calculations in slab geometry. The radial bucklings came from two-dimensional calculations. The cross-sections were heterogeneity corrected. In this case the heterogeneity code KAPER was used, which takes into account the anisotropic diffusion. Fig. 11 shows the experimental and calculated results. One notes that the calculations overestimate the diffusion term but one notes too, that the difference in the sodium void effect for different platelet orientations is interpreted well by the calculations.

8.2 Sodium void effect of large sodium void zones

8.2.1 Description of the experiments

Measurements of central void zones of increasing radius have the aim of approaching the maximum possible positive void effect.

The voided zones had a height of 60.84 cm (centered on the midplane). This height corresponds roughly to the maximum axial sodium void effect. The number of voided core elements was enlarged stepwise from four elements to 112 elements. Fig. 12 shows the core cross-sections of the core with each void zone and gives the cylindrical radii of the voided zones.

8.2.2 Description of the calculational methods

A detailed description of the evaluation and the calculational methods used will be given in /13/. The basic calculations were two-dimensional exact perturbation calculations in R-Z-geometry. Two cross-section-sets, MOXTOT and KFKINR, were used. The cross-sections were heterogeneity corrected with the code ZERA. The influence of the anisotropic diffusion was estimated with one-dimensional perturbation calculations. In these calculations cross-sections were used which were heterogeneity corrected with the KAPER-code.

The transport correction was calculated by the comparison of two-dimensional calculations performed with the transport code SNOW and the diffusion code DIXY. Also, a REMO-correction (for the elastic removal cross-sections) was found and added to the calculated results. Fig. 13 gives the experimental and the calculated final results. One notes that the results calculated with the KFKINR-set show a good agreement with the experiments. The calculations performed with the MOXTOT-set underestimate the Na-void effect. The cause of this underestimation is a large REMO-correction.

9. Doppler reactivity measurements

9.1 Description of the experiments

The Doppler effect of ^{238}U and ^{239}Pu was measured at the core center, using the technique of oscillating a hot versus a cold sample in the pile oscillator. The changes in reactivity were obtained by the inverse kinetics method. The experiments were carried out at 15 W reactor power, the typical error was 3×10^{-5} %.

Two samples were used for the measurements. One was a depleted UO_2 sample (877.9 g UO_2 , 0.4% ^{235}U), the other one was a PuO_2 sample, diluted with Al_2O_3 (451.7 g PuO_2 , 7% ^{240}Pu). The dilution of the PuO_2 sample with Al_2O_3 has the advantage that the reactivity effect due to thermal expansion is very small, and that there is no strong flux dip in the resonance region inside the sample. Both samples were heated electrically up to 700°C . The samples and the experimental technique are described in more detail in /14/.

The results are shown in Fig. 14. The UO_2 sample shows a fairly strong negative reactivity effect upon heating, whereas the effect for the PuO_2 sample is very small, but it is clearly negative for large temperature changes. The data point for the UO_2 sample were fitted to the expression

$$\delta k/k = -A \ln T/T_0,$$

in order to obtain an experimental Doppler constant, $A = 7.65 \times 10^{-6}$ $\delta k/k / \text{kg } ^{238}\text{U}$.

9.2 Comparison with calculations

The interpretation of the Doppler sample measurements is complicated because of the interaction effect between the "hot" resonances in the sample and the "cold" resonances in the environment. This effect can be calculated with the program DOPRU, which is based on a perturbation solution of the integral transport equation /15/. On the

other hand, the Doppler effect in a fast reactor can be calculated by standard multigroup diffusion calculation, using the self-shielding factors at different temperature, or by the Doppler modul included in the NUSYS program system, and it is desirable to compare the measurements also to these standard calculations.

Therefore, the interpretation of the measurements with the UO_2 samples was carried out as follows: Two DOPRO calculations were run, one for the actual experimental configuration, and one for the case where the interaction terms were omitted, i.e. the self-shielded cross-sections of the sample, calculated with the equivalence theorem, were used. A difference of +2.8% between the two cases was found, and applied as a correction to the experimental results.

For comparison with calculations, one can normalize the Doppler effect to the central worth of ^{239}Pu , in order to eliminate the reactivity scale.

The comparison for both the Doppler constant A, and the ratio A/worth of ^{239}Pu is shown in the Table 10.

Note that all the calculations use the same flux and adjoint spectrum, which was obtained from a diffusion calculation with the KFKINR-cross-section-set. Thus, the only difference is in the method, and the resonance data used to calculate the Doppler changes of the self-shielded cross-sections. DOPRO uses the data from the data file KEDAK except that the p-wave strength function S_1 was modified. The value 1.75×10^{-4} was taken from a recent evaluation by Pitterle and Durston /16/, and the value 1.5×10^{-4} may be considered as a lower limit. Table 10 shows that the DOPRO results are rather sensitive to the value assumed for S_1 . The two most

reliable calculations, with DOPRO ($S_1 = 1.75 \times 10^{-4}$) and with KFKINR are in good agreement, though they underestimate the experimental result by 20%. This underestimation is not explained yet. However, it is similar to the results reported by the Argonne group /17/.

It is interesting to note that much better agreement was obtained for earlier SNEAK-measurements in core composition typical of steam-cooled reactors, where the underestimation was only about 10% /14/. A likely explanation for this difference is that in a steam-cooled reactor, most of the Doppler effect occurs at low energies, where the resonance parameters are resolved, and well known.

The measurements with the PuO_2 sample were analyzed only with the DOPRO program. The reactivity effect due to thermal expansion was also calculated, but found to be small (Fig. 14). Though experiment and calculation give values of opposite sign, the absolute deviation (reactivity per g of material) is only about twice as large as for the UO_2 sample. In view of the strong compensation between fission effect and absorption effect, this larger difference is not surprising.

Acknowledgements

The author gratefully acknowledges the valuable help from R. Kiesel and M. Mäule as well as the steady cooperation of the SNEAK operation group.

References

- /1/ F. Helm et al.
Physics Investigations of Sodium Cooled Fast Reactors.
SNEAK-Assembly 2
KFK-1399 (June 1971)
- /2/ G. Jourdan et al.
Physics Investigations of Sodium Cooled Fast Reactors.
SNEAK-Assemblies 6A/6B
KFK-1612 (June 1972)
- /3/ E. Kiefhaber, J.J. Schmidt
Evaluation of Fast Critical Experiments Using Recent
Methods and Data
KFK-969 (September 1970)
- /4/ E. Kiefhaber
The KFKINR-Set of Group Constants; Nuclear Data Basis and
First Results of its Application to the Recalculation of
Fast Zero-Power Reactors
KFK-1572 (March 1972)
- /5/ D. Wintzer
Zur Berechnung von Heterogenitätseffekten in periodischen
Zellstrukturen thermischer und schneller Kernreaktoren
KFK-743 (Januar 1969)

- /6/ P.E. Mc Grath
KAPER - Lattice Program for Heterogeneous Critical
Facilities (User's Guide)
KFK-1893 (December 1973)
- /7/ H. Huschke et al.
Zur Berechnung des Neutronenflusses in sehr vielen (208)
Energiegruppen
KFK-1270/2, Chapter 1222.2
- /8/ H. Küsters et al.
The Group Cross Section Set KFK-SNEAK; Preparation and
Results
KFK-608 (October 1967)
- /9/ C. Günther, W. Kinnebrock
Das eindimensionale Transportprogramm DTK
KFK-1381 (März 1971)
- /10/ C. Günther, W. Kinnebrock
SNOW - Ein zweidimensionales S_N -Programm zur Lösung der
Neutronentransportgleichung in Platten- und Zylinder-
geometrie
KFK-1826 (Juli 1973)
- /11/ A. Meyer-Heine et al.
BNES Conference paper 1.2
London (June 1969)
- /12/ P. Hammer, CEN de Cadarache - private communication (1971)

- /13/ G. Jourdan
KFK-report will be published
- /14/ L. Barleon, E.A. Fischer
Small-Sample Doppler Effect Measurements and their Interpretation in Fast Reactor Spectra
Nuclear Science and Engineering 47 (1972) p. 247-261
- /15/ E.A. Fischer
Interpretation of Doppler Coefficient Measurements in Fast Critical Assemblies
ANL-7320 (1966) p. 350
KFK- 844 (May 1969)
- /16/ Report on the EANDC Specialist Meeting at Harwell
EANDC-90 "L" (1972)
- /17/ C.E. Till
The Fast Neutron Doppler Effect
Meeting on New Developments in Reactor Physics and Shielding, CONF-720901 (1972)

Table 1a Atomic compositions (10^{22} at/cm³) SNEAK-9B plutonium zone

Isotopes	Compositions of the pure cells (used for reaction rate calculations)			Compositions used for the k_{eff} calculations			
				Central core zone		Outer Pu-zone	
	Pu-zone	control rods	ax.breeder blanket	core zone	ax.breeder blanket	core zone	ax.breeder blanket
Al	.00037	.95583	.26146	.01417	.26146	.10111	.27591
Au	.00153			.00152		.00138	
Am	.00030			.00029		.00027	
C	.00431	1.05458	.00453	.00429	.00453	.10125	.03125
Cr	.28127	.28894	.25592	.28008	.25592	.28090	.25829
Fe	.99592	1.04657	.90738	.99172	.90738	.99678	.91776
H		.00237	.00061		.00061		.00075
Mg	.00016	.00979	.00289	.00031	.00289	.00118	.00301
Mn	.01207	.02099	.01256	.01210	.01256	.01292	.01314
Mo	.00217		.00196	.00216	.00196	.00196	.00177
Na	1.02567	.64009	.66527	1.01849	.66527	.98355	.65710
Ni	.17182	.15351	.14386	.17102	.14386	.16940	.14490
O	1.00773	.96809	1.39792	1.00068	1.39792	.99767	1.34950
Pu-239	.12166			.12080		.10965	
Pu-240	.01093			.01085		.00985	
Pu-241	.00081			.00081		.00073	
Pu-242	.00005			.00005		.00004	
Si	.01388	.01991	.01445	.01393	.01445	.01448	.01451
Ti		.00388				.00036	.00036
U-234	.00002			.00002		.00001	
U-235	.00393	.15167	.00499	.00390	.00499	.01755	.00498
U-238	.66876	.60526	.68833	.66408	.68833	.65864	.68725

Table 1b Atomic compositions (10^{22} at/cm³) SNEAK-9B uranium zone and radial blanket

Isotopes	Uranium zone					Radial blanket
	Compositions of the pure cells (used for reaction rate calculations)			Compositions used for the k_{eff} calculations		
	uranium zone	control rods	ax.breeder blanket	core zone	ax.breeder blanket	
Al		.94098	1.27370	.08553	1.09838	.45420
C	1.45897	1.45650	.00875	1.45966	.00791	.00016
Cr	.24091	.24842	.26338	.24161	.25677	.13314
Fe	.85686	.90028	1.11583	.86088	1.06972	.47000
H	.00119	.00106	.00061	.00117	.00053	
Mg		.00964	.01325	.00087	.01143	
Mn	.01182	.02001	.01702	.01256	.01685	.00926
Mo	.00171		.00139	.00155	.00120	
Na	1.13846	.28768		1.06136		
Ni	.14768	.13467	.92611	.14649	.09689	.0480
O	.45872	.43509	1.39354	.45685	1.20173	
Si	.01159	.01812	.02167	.01218	.01991	.00155
Ti		.00388		.00035	.00053	.00005
U-235	.23979	.23987	.00498	.23957	.00623	.01624
U-238	.43933	.44009	.68618	.43898	1.06932	3.99400

Table 2 Compositions of the homogenized absorbers (step Nr. 4)

10^{22} at/cm ³	Alu	B ₄ C	Eu ₂ O ₃	Ta
Al	5.24500	3.06670	3.06450	3.09070
B-10	--	.40419	--	--
B-11	--	1.65700	--	--
C	.00136	.51664	.00136	.00136
Cr	.12041	.12041	.12041	.12041
Eu	--	--	.07909	--
Fe	.39594	.39594	.39594	.39594
Mo	.00010	.00010	.00010	.00010
Ni	.05723	.05723	.05723	.05723
O	--	--	.00119	--
Si	.00453	.00453	.00453	.00453
Ta	--	--	--	1.68860

Table 3 Atomic compositions (10^{22} at/cm³)
SNEAK-9B composition of the voided
zone (normal cell)

Isotopes	
Al	.00037
Au	.00153
Am	.00029
C	.00465
Cr	.27918
Fe	.98568
Mg	.00016
Mn	.01185
Mo	.00218
Ni	.17115
O	1.00861
Pu-239	.12176
Pu-240	.01094
Pu-241	.00081
Pu-242	.00005
Si	.01473
U-234	.00002
U-235	.00393
U-238	.66935

Table 4 Atomic compositions (10^{22} at/cm³)
SNEAK-9B composition of the special
cell for axial sodium void measurements

Isotopes	Normal cell	Voided cell
Al	.00038	.00038
Au	.00155	.00155
Am	.00030	.00030
C	.00435	.00470
Cr	.28392	.28181
Fe	1.00526	.99486
Mg	.00017	.00017
Mn	.01212	.01190
Mo	.00218	.00220
Na	1.04162	
Ni	.17200	.17133
O	1.02340	1.02430
Pu-239	.12355	.12366
Pu-240	.01110	.01111
Pu-241	.00083	.00083
Pu-242	.00005	.00005
Si	.01403	.01489
U-234	.00002	.00002
U-235	.00374	.00374
U-238	.61791	.61846

Table 5 Atomic compositions¹⁾ (10^{22} at/cm³) of SNEAK-platelets used in Na-void measurements

Isotopes	PuO ₂ UO ₂	Na	U _{depl}	Empty can
Al	.00120			
Am	.00096			
C	.00621	.00372	.00136	.00427
Cr ²⁾	.28902	.31713	.11955	.31341
Fe	.98351	1.07686	.39549	1.06032
Ni	.14772	.18539	.15978	.18432
O	3.26959			
Pu-239	.39472			
Pu-240	.035459			
Pu-241	.00205			
Pu-242	.00016			
Si	.01156	.01621	.00453	.01759
U-235	.00877		.01604	
U-238	1.19139		3.93893	
Au	.00496			
Na		1.66712		
Geometry				
square (cm ²)	5.44x5.44	5.44x5.44	5.44x5.44	5.44x5.44
height (cm)	.6260	.6248	.1555	.6239

1) These numbers include the composition of the tubes

2) Mn has been added to Cr

Table 6 Results of the k_{eff} calculations for SNEAK-9B

	MOXTOT	KFKINR
2-d hom. diffusion calculation	.9926	1.0026
Correction for cylindrization	-.0022	-.0021
Heterogeneity correction	+.0003	-.0006
Transport correction (S_6) 2-d calculated with the SNOW-code	+.0059 ⁺⁾	+.0059
REMO correction	+.0039	+.0007
Final results	1.001	1.006

⁺⁾ This result is taken from MOXTOT-set

Table 7 Results of the evaluation of the material worth measurements in SNEAK-9B

Isotopes	Weight of the probe (g)	Exp. result (m\$/g)	C/E
U-235	6.69	.490 ± .01	1.093
U-238	123.6	-.0295 ± .006	.975
Pu-239	4.04	.661 ± .015	1.103
Pu-240	2.7	.132 ± .013	1.03
Pu-241	1.28	1.006 ± .05	.98
B-10 (90% B-10 in the probe)	.589	-9.90 ± .1	.963
B-10 (B ₄ C probe)	6.26	-10.87 ± .1	.909
B ₄ C	6.26	-1.545 ± .02	.909
Na	29.9	-.0315 ± .0015	1.30 ^{a)}
Cf		.209 (m\$/cm ³) ^{b)}	1.12

β_{eff} used in the calculations = $442.8 \cdot 10^{-5}$

- a) This value is very sensitive to the treatment of heterogeneity. This explains the inconsistency with the evaluation of the Na-void measurements. Further analysis of this problem is in progress.
- b) This result is based on a calibration of the ²³⁹Pu fission chamber performed in April 1974

Table 8 Results of the buckling evaluation in SNEAK-9B

Experimental	$\alpha \text{ (m}^{-1}\text{)}$	2.417 ± 0.003
	$\beta \text{ (m}^{-1}\text{)}$	2.930 ± 0.006
	$B_m^2 = \alpha^2 + \beta^2$	14.69 ± 0.04
Calculated	KFKINR	15.32
	MOXTOT	14.72

Table 9a Results of the absorber worth evaluation (central core position, normal core)

$\Delta k/k$ (m%)		Step 1	Step 2	Step 3	Step 4
$\beta_{\text{eff}} = 442.8 \cdot 10^{-5}$		4 small absorber rodlets	4 small + 4 big absorber rodlets	4 small + 8 big absorber rodlets	8 small + 8 big absorber rodlets
B_4C	Calculations	- 109	- 407	- 660	- 753
	Experiment	- 111	- 408	- 673	- 766
	C/E	.98	1.00	.98	.98
Ta	Calculations	107	--	- 606	- 678
	Experiment	- 98	- 346	- 562	- 638
	C/E	1.09	--	1.08	1.06
Eu_2O_3	Calculations	- 19	--	- 95	- 98
	Experiment	- 20	- 77	- 128	- 146
	C/E	.95	--	.74	.67

Reference core: core with Al-matrix

Error of the measurements: ± 2 m%

Table 9b Results of the absorber worth evaluation (central core position, voided zone)

$\Delta k/k$ (m%) $\beta_{\text{eff}} = 442.8 \cdot 10^{-5}$	B_4C	Ta	Eu_2O_3
Calculations	- 612	- 569	- 55
Experiments	- 628	- 528	- 97
C/E	.97	1.08	.57

Reference core: core with Al-matrix

Error of the measurements: ± 2 m%

Table 9c Results of the absorber worth evaluation (eccentric position, normal and voided core)

$\Delta k/k$ (m β) $\beta_{\text{eff}} = 442.8 \cdot 10^{-5}$	Normal core			Voided core		
	B_4C	Ta	Eu_2O_3	B_4C	Ta	Eu_2O_3
Calculations	- 540	- 485	- 94	- 493	- 449	- 69
Experiments	- 557	- 464	- 115	- 490	- 410	- 91
C/E	.97	1.05	.82	1.01	1.09	.76

Reference core: core with Al-matrix

Error of the measurements: ± 2 m β

Table 9d Results of the absorber worth evaluation (worth of the Al-matrix in all positions, normal and voided core)

$\Delta k/k$ (m\$)	Normal core		Voided core	
	Position		Position	
	central	excentric	central	excentric
$\beta_{\text{eff}} = 442.8 \cdot 10^{-5}$				
Calculations	319	229	334	242
Experiments	317	203 ⁺⁾	334	231
C/E	1.01	1.13	1.00	1.05

⁺⁾ uncertain value

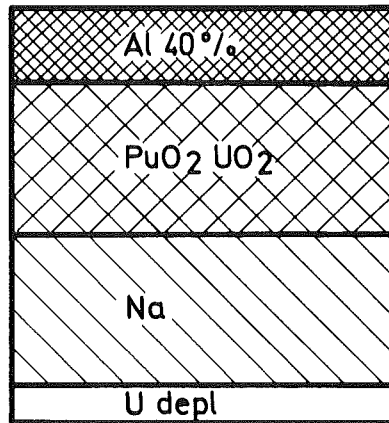
Error of the measurements: ± 2 m\$

Table 10

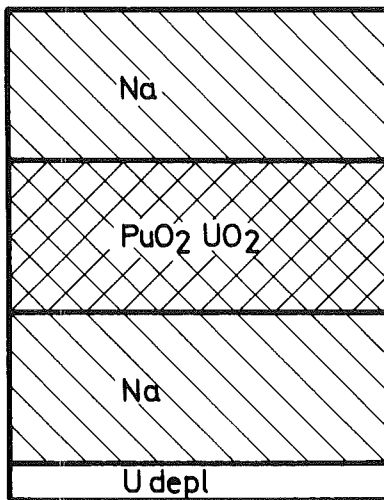
Comparison of the Doppler measurements in depleted UO₂ with calculations

	Doppler constant A $10^{-6} \frac{\delta k}{k} / \text{kg } ^{238}\text{U}$	C/E	
		A	$\frac{A}{\text{worth of } ^{239}\text{Pu}}$
Experiment, corrected for interaction terms	7.85		
<u>Calculations</u>			
DOPRO, $S_1 = 1.50 \times 10^{-4}$	6.72	0.855	0.78
DOPRO, $S_1 = 1.75 \times 10^{-4}$	6.99	0.89	0.81
KFKINR with f-factors for different temperatures	6.91	0.88	0.80
DOPPLER modul in NUSYS	8.17	1.04	0.94

upper rest cell



normal cell



lower rest cell

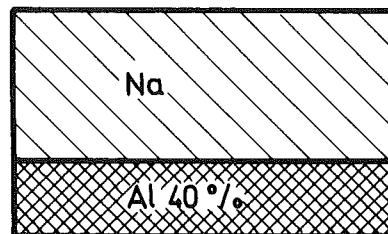
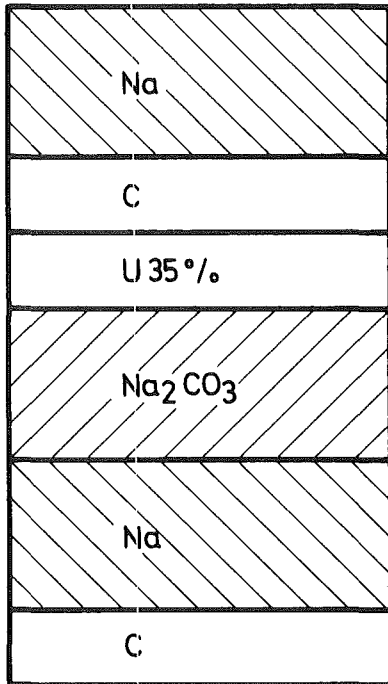
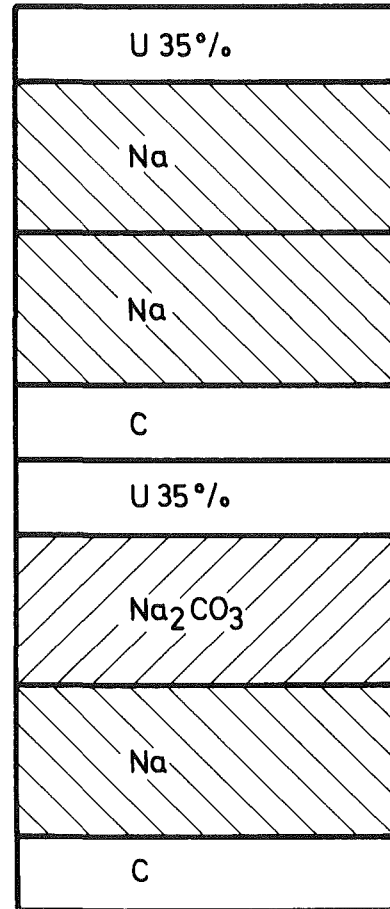


Fig.1a Cells of the Normal Core Elements
(Pu - Zone)

upper rest cell



normal cell



lower rest cell

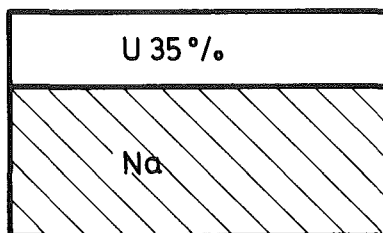
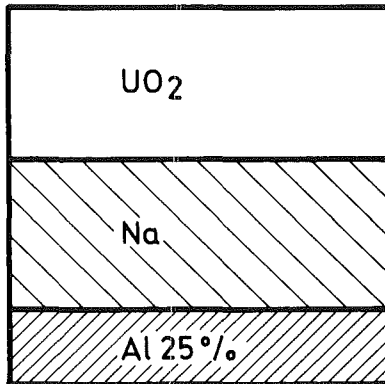


Fig. 1b Cells of the Normal Core Elements
(Uranium - Zone)

Pu - zone



Uranium - zone

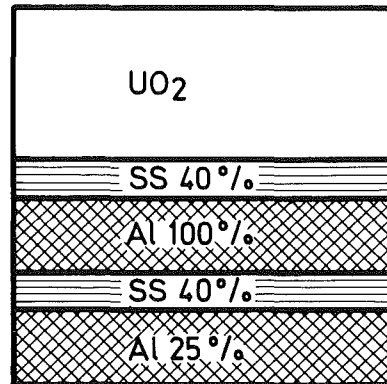


Fig.1c Cells of the Axial Breeder Blanket
(Core Elements)

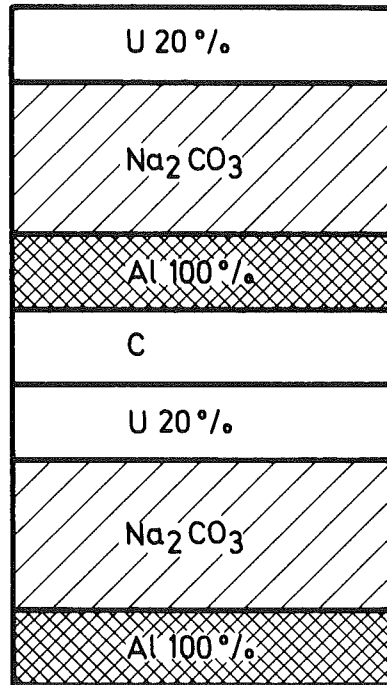
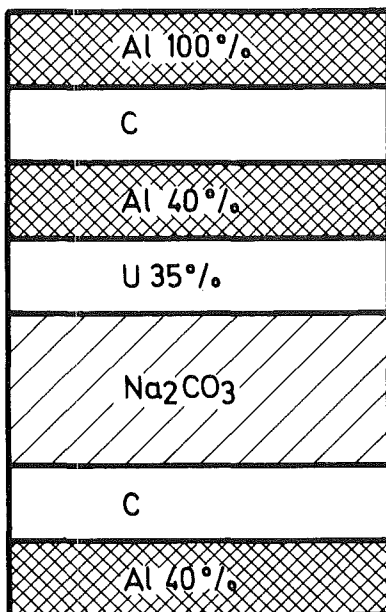
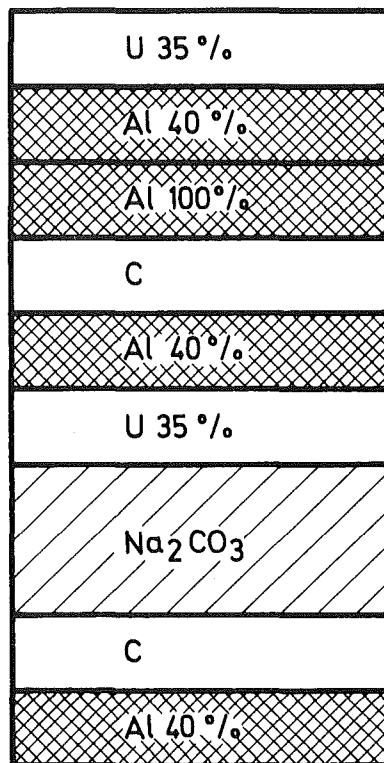


Fig. 2a Cell of the Control - Rods (Shim - and
Safety - Rods)
(Pu - Zone)

upper rest cell



normal cell



lower rest cell

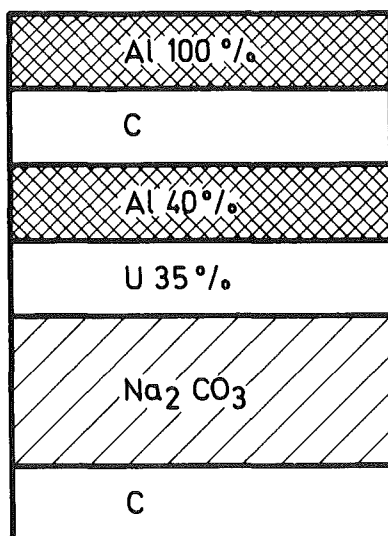
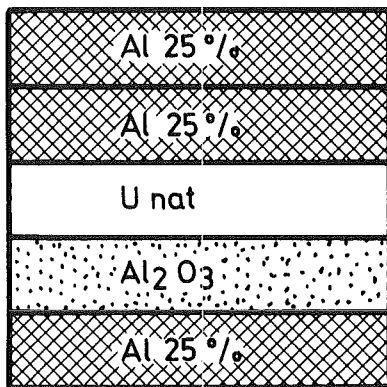


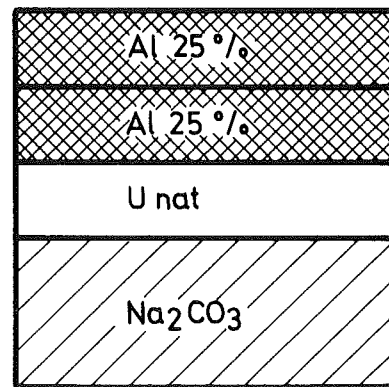
Fig. 2b Cells of the Control - Rods (Shim - and Safety - Rods)
(Uranium - Zone)

Pu - zone

Shim - rod



Safety - rod



Uranium - zone

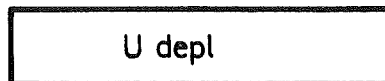
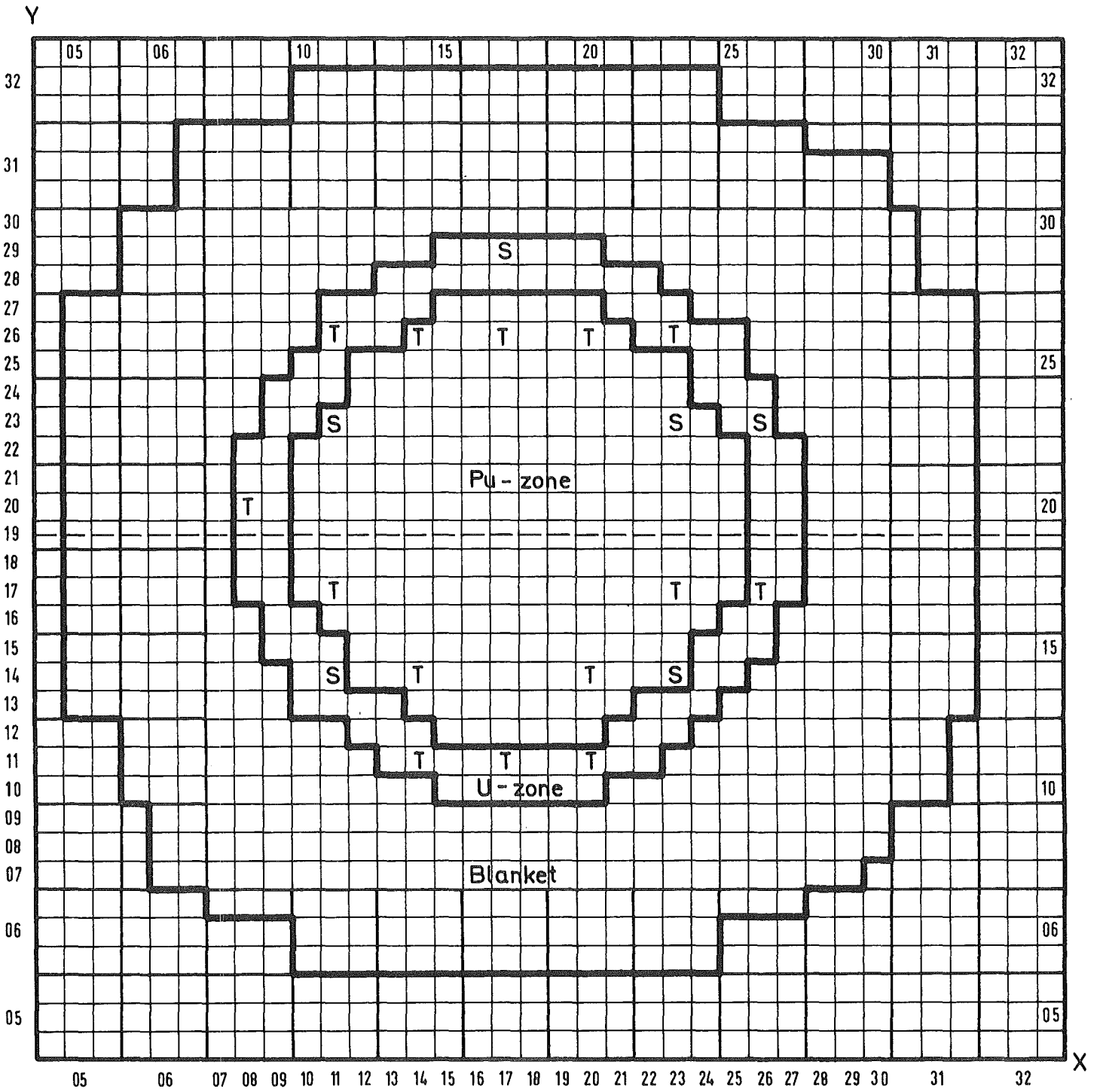


Fig. 2c Cells of the Axial Breeder Blanket for the Control - Rods



SNEAK-9B Cross Section of the Critical Configuration

S = Safety rod
T = Shim rod
--- = Radial channel

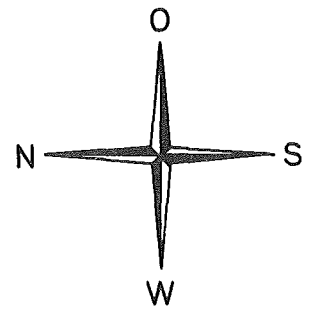


Fig.3

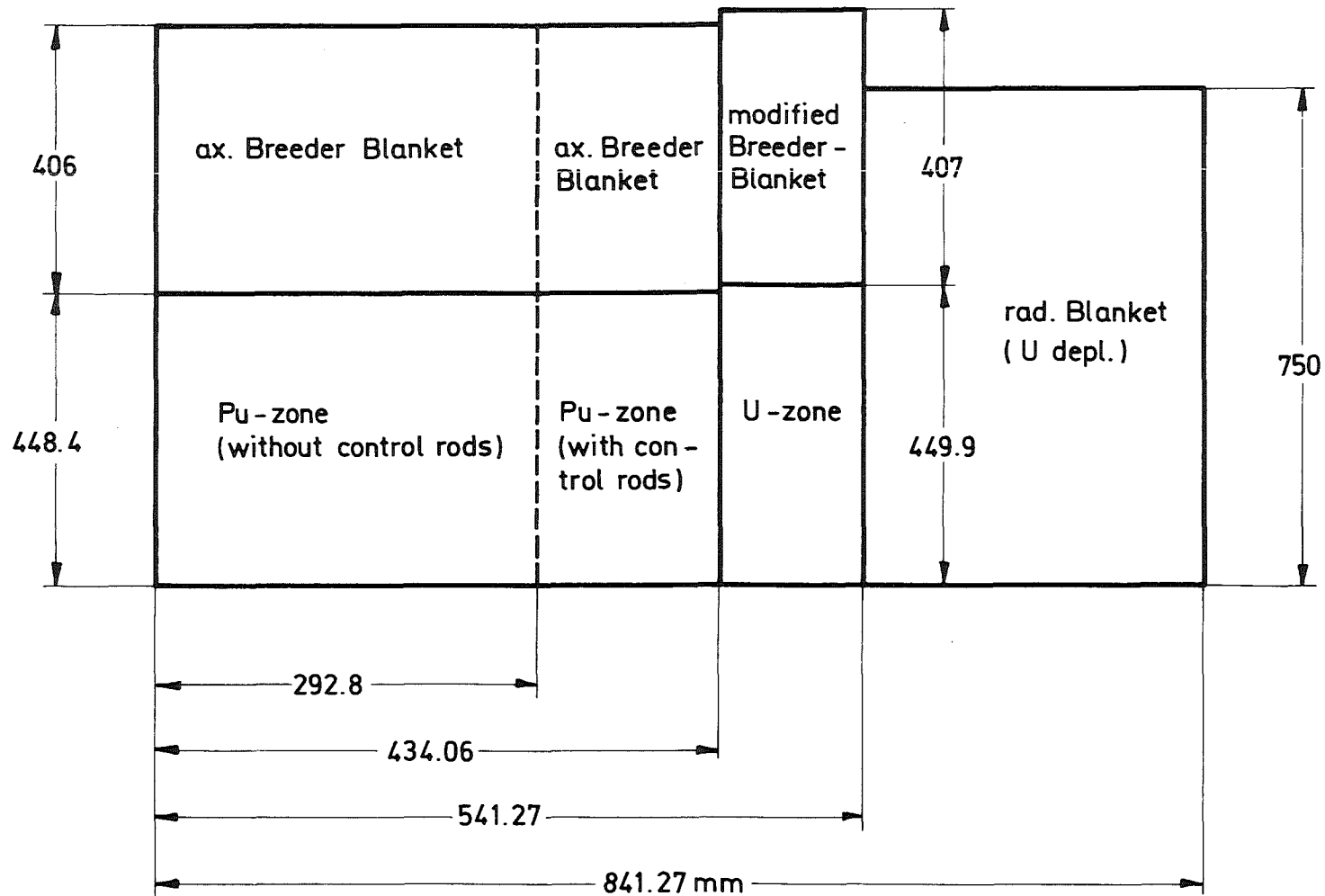


Fig.4 Axial Cut through a Quarter of the Critical Configuration

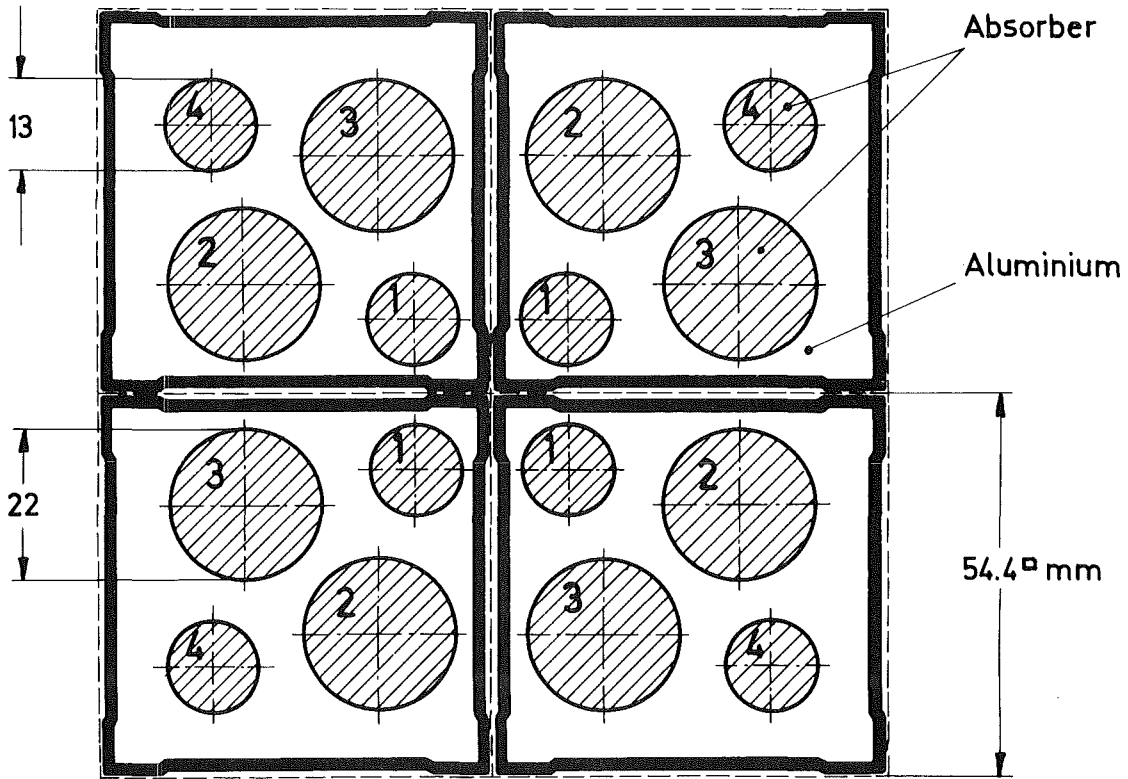
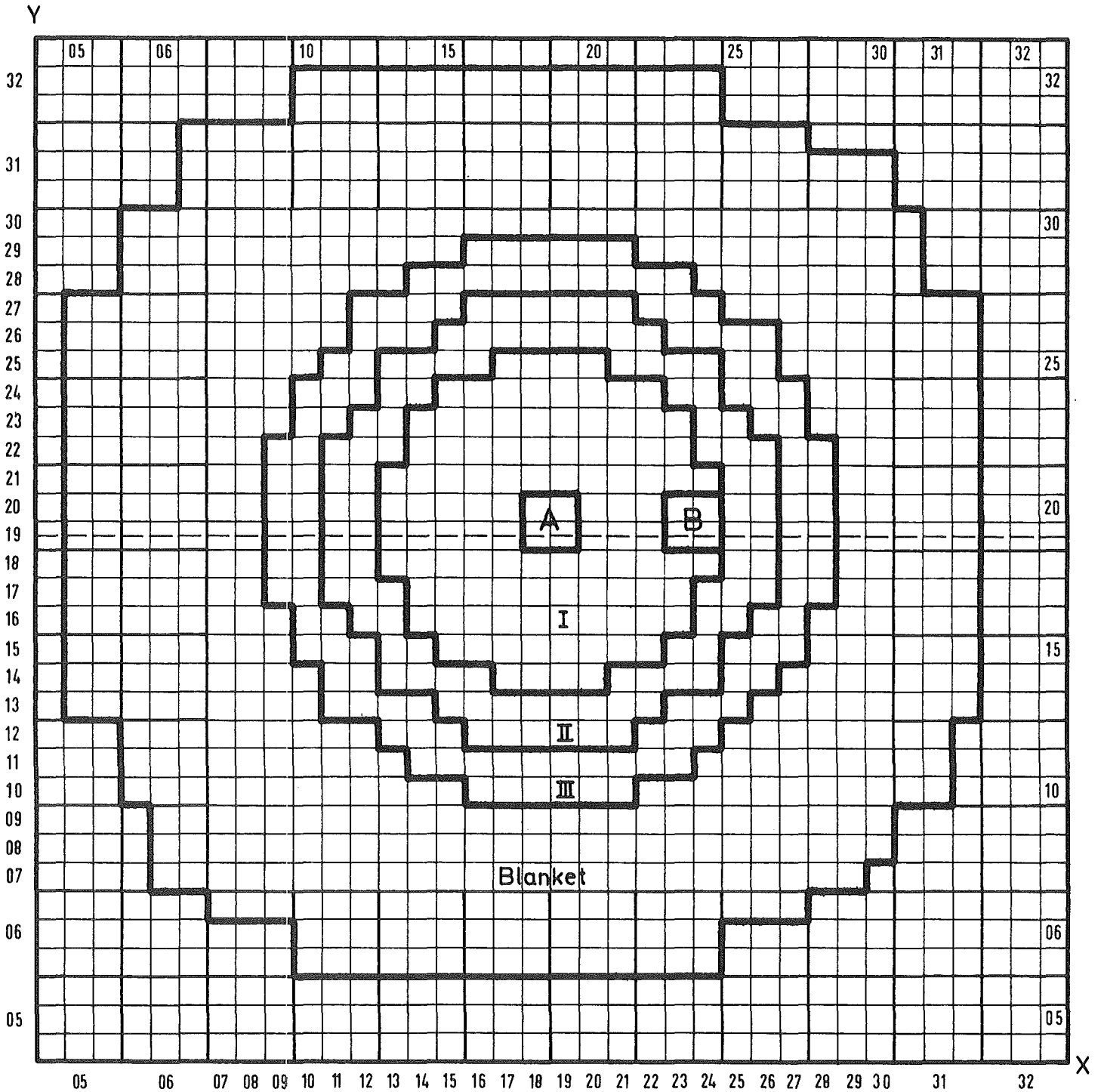


Fig.5 Cross Section of the Absorber - Zone in SNEAK - 9B

(The Numbers in the Absorber - Holes gives the Step - Number of the Measurements)



SNEAK - 9B Positions of the Absorber Zones

- I Normal or voided Pu-zone
- II Pu-zone (not voided)
- III Uranium - zone



Central position of the absorber zone



Eccentric position of the absorber zone

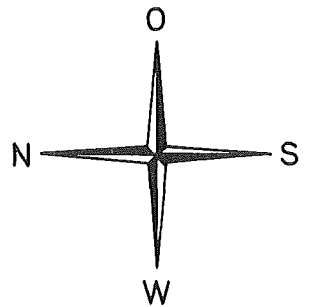
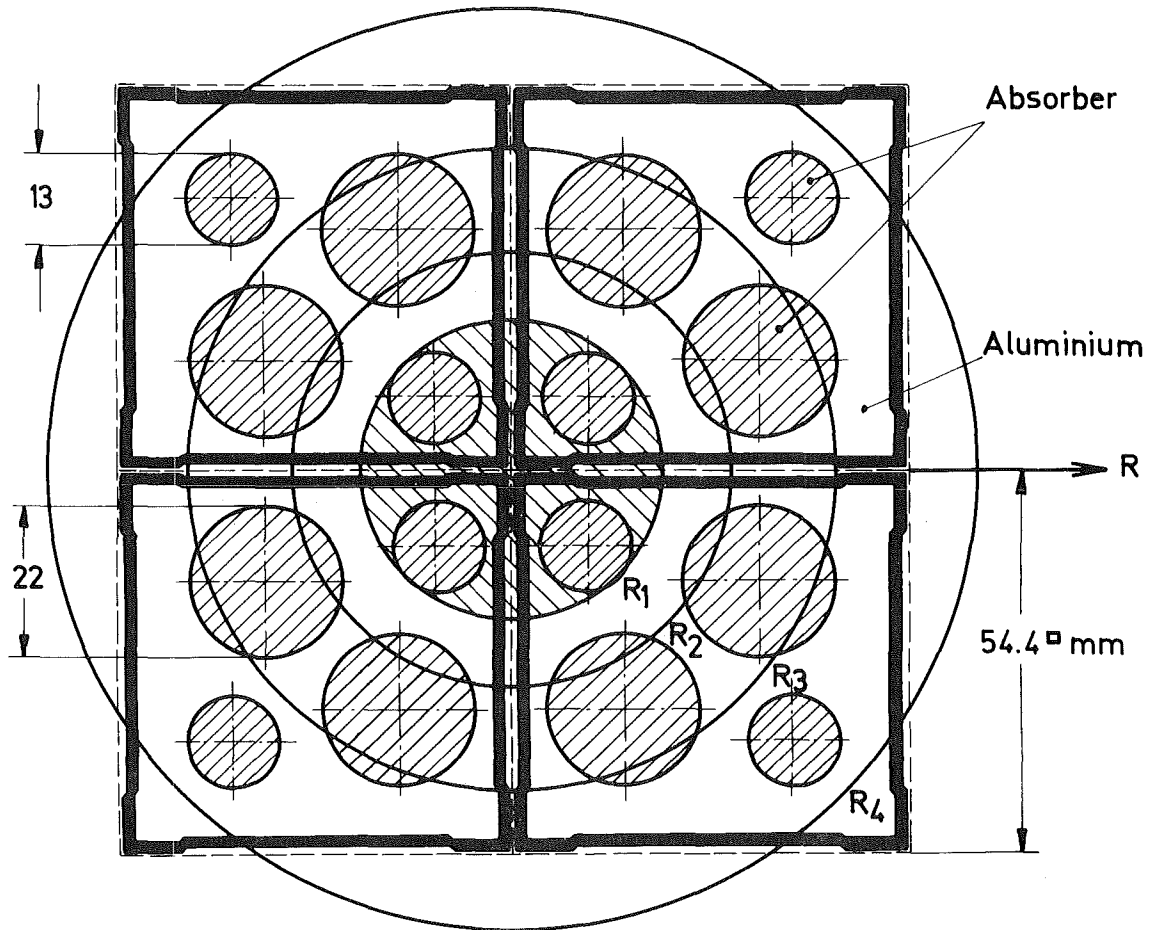


Fig. 6



- R₁ = 1.85 cm
- R₂ = 3.6 cm
- R₃ = 4.8 cm
- R₄ = 6.14 cm

Fig.7a Models for the Absorber Calculations
(Cylindrical Model)

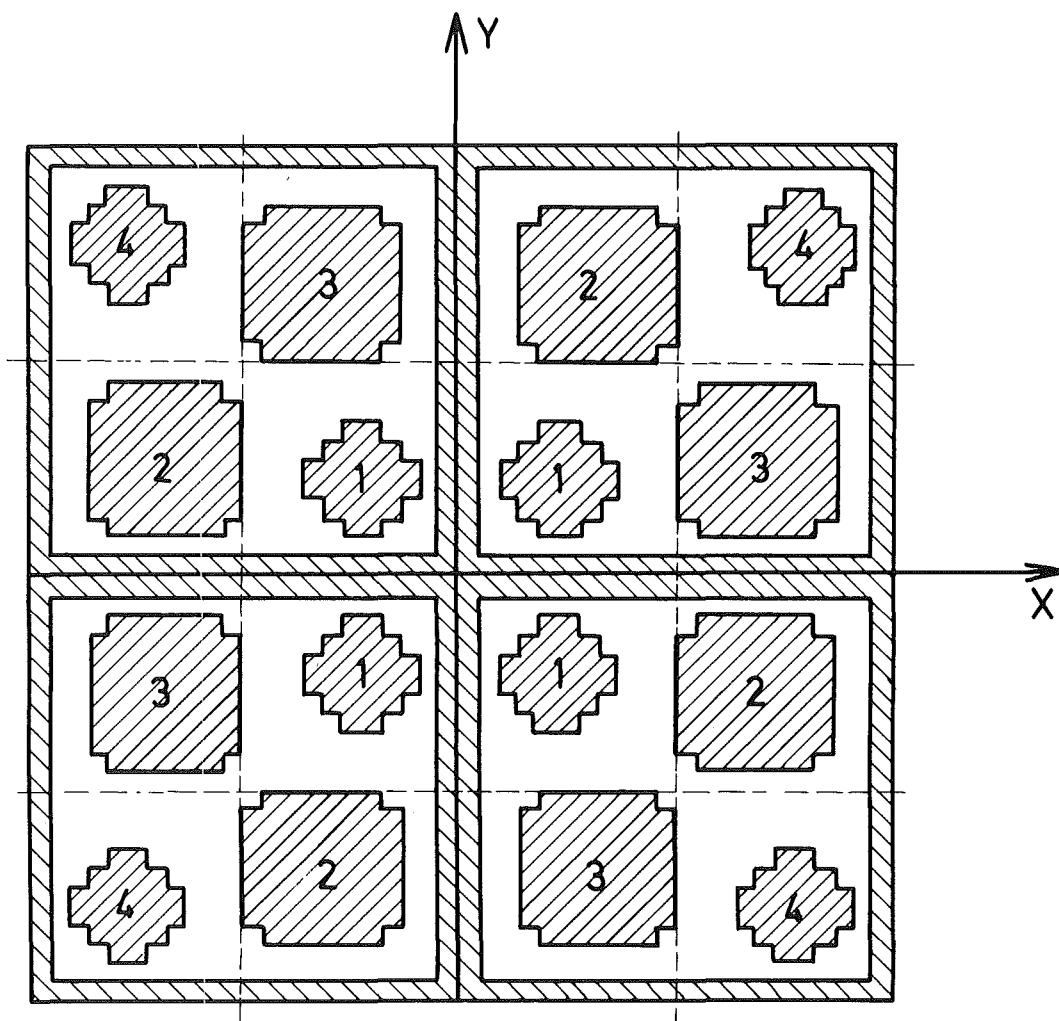


Fig. 7b Models for the Absorber Calculations
(Polygons Model)

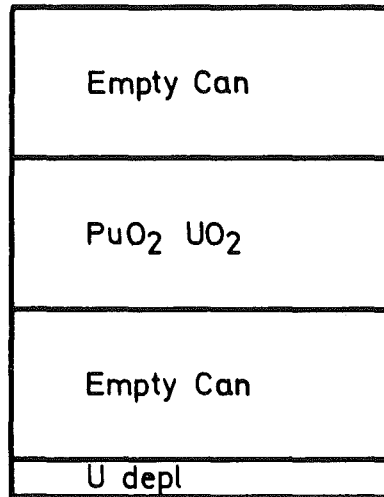
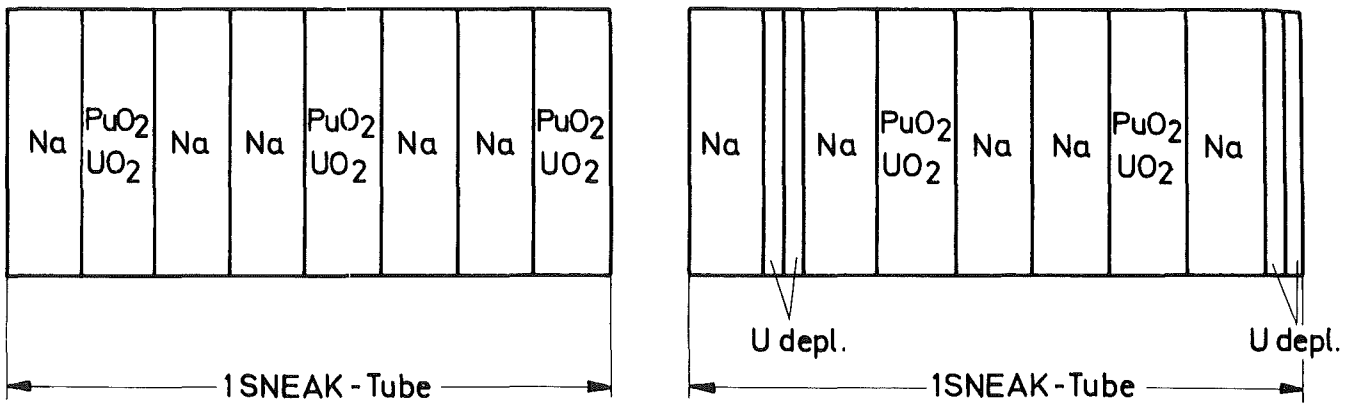
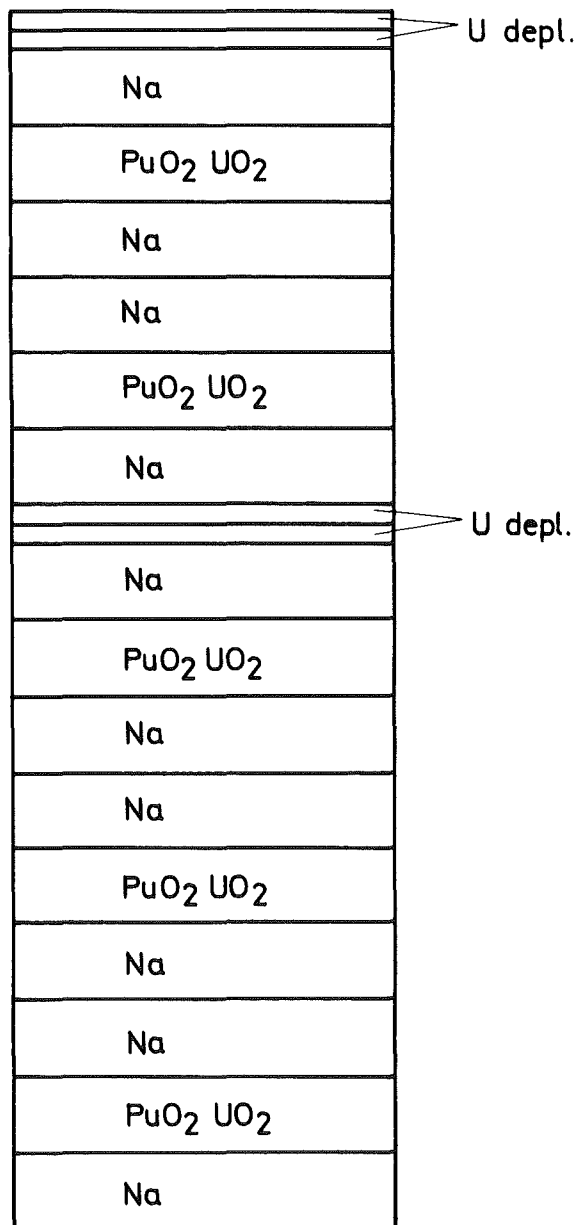


Fig. 8 Normal -Cell for the Na - Void Measurements
(In Axial and Radial Direction)



A) Platelets in vertical position



B) Platelets in horizontal position

Fig.9 Modified Cell for Axial Na-Void Measurements

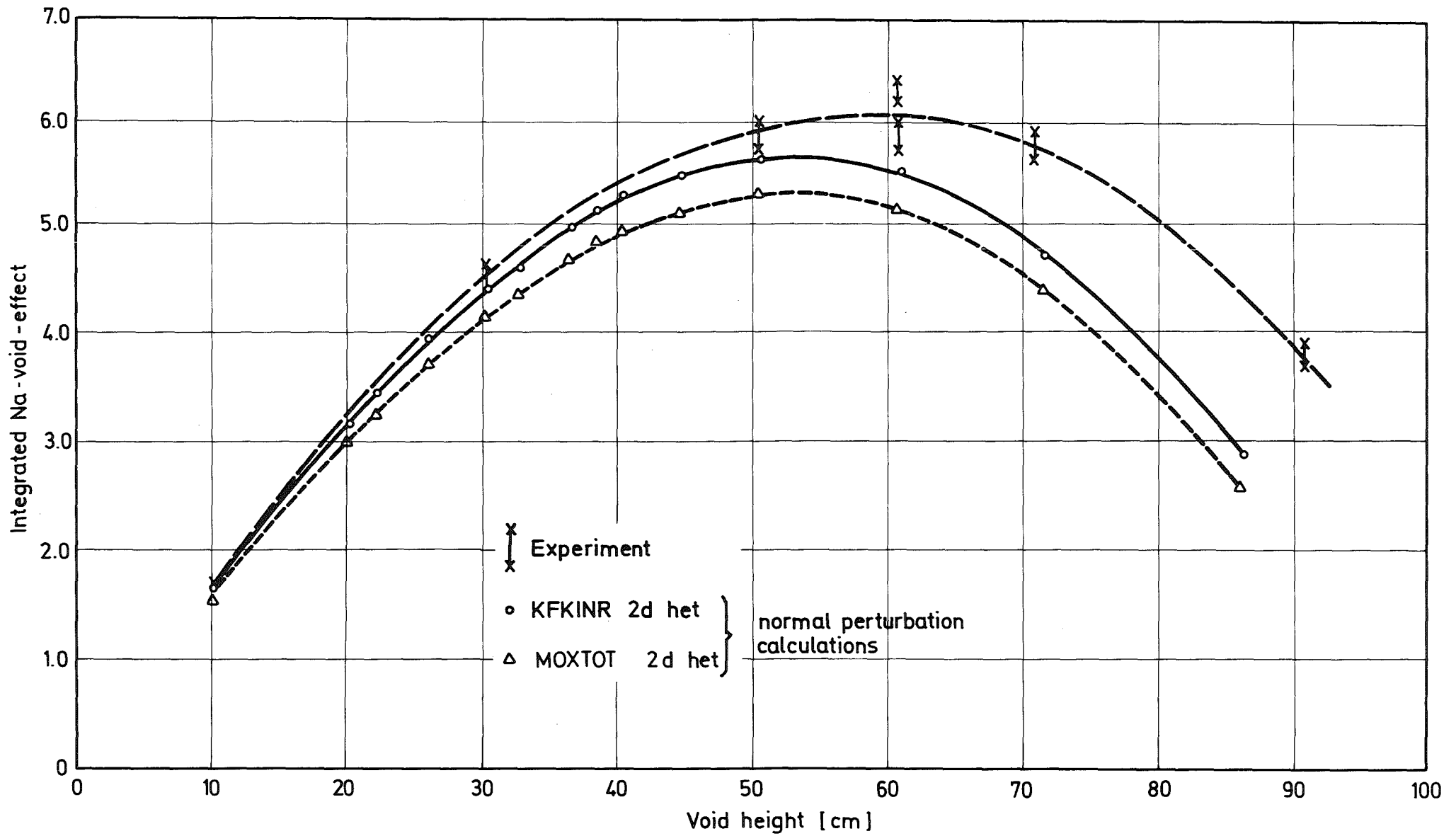


Fig.10 Integrated Axial Na-Void Effect for the Normal Cell SNEAK-9B

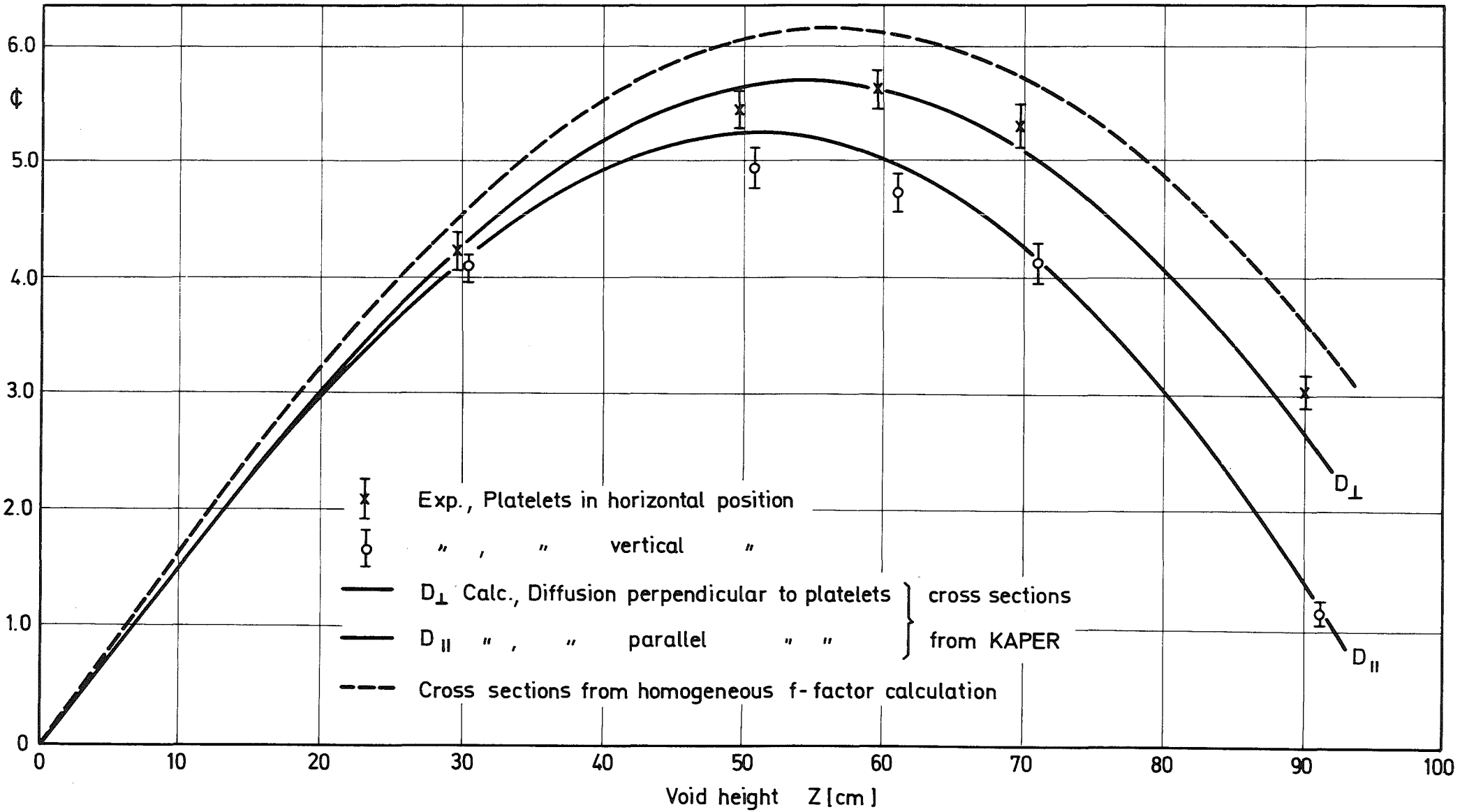
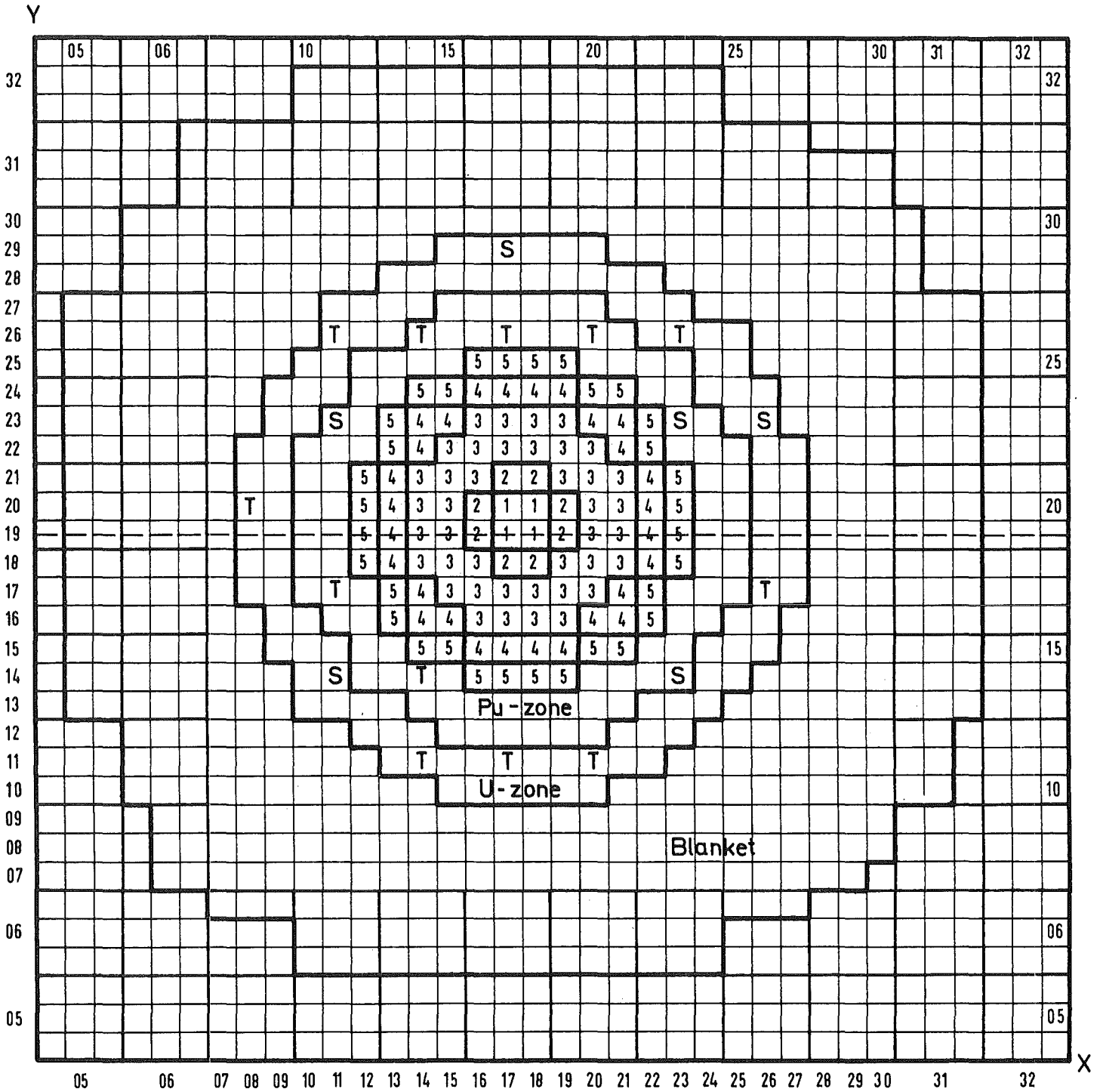
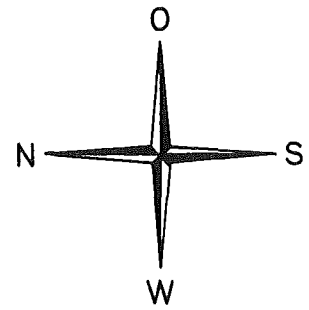


Fig.11 Integrated Axial Sodium Void Reactivity Effect for Different Platelet Orientations, SNEAK - 9B



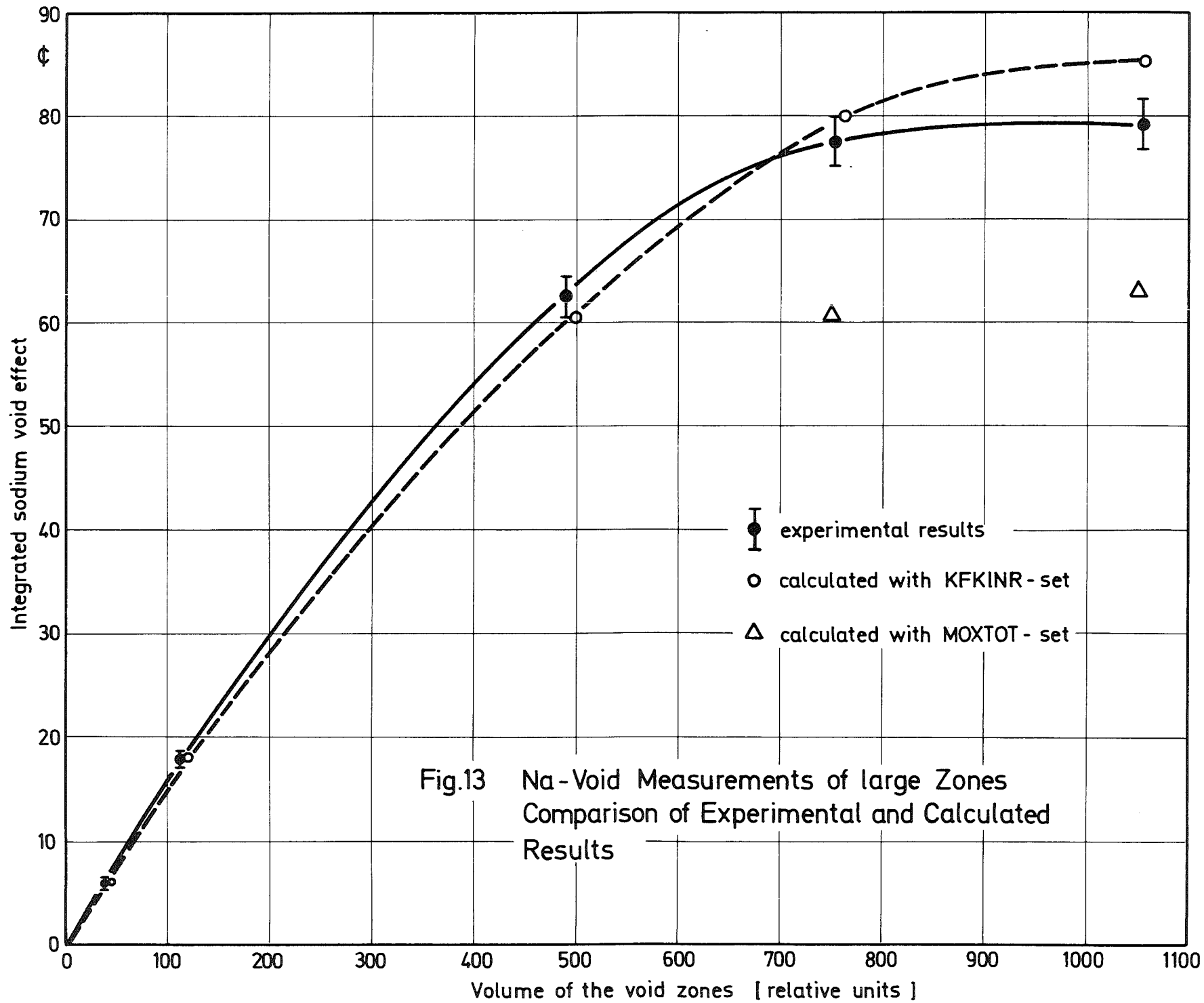
SNEAK-9B Radial Na-Void Measurements
Cross Section of the Core with
Void Configurations



Step	Number of elements voided	cylindrical
1	4	6.14
2	12	10.63
3	52	22.13
4	80	27.45
5	112	32.48

Fig. 12

T = shim rods
S = safety rods



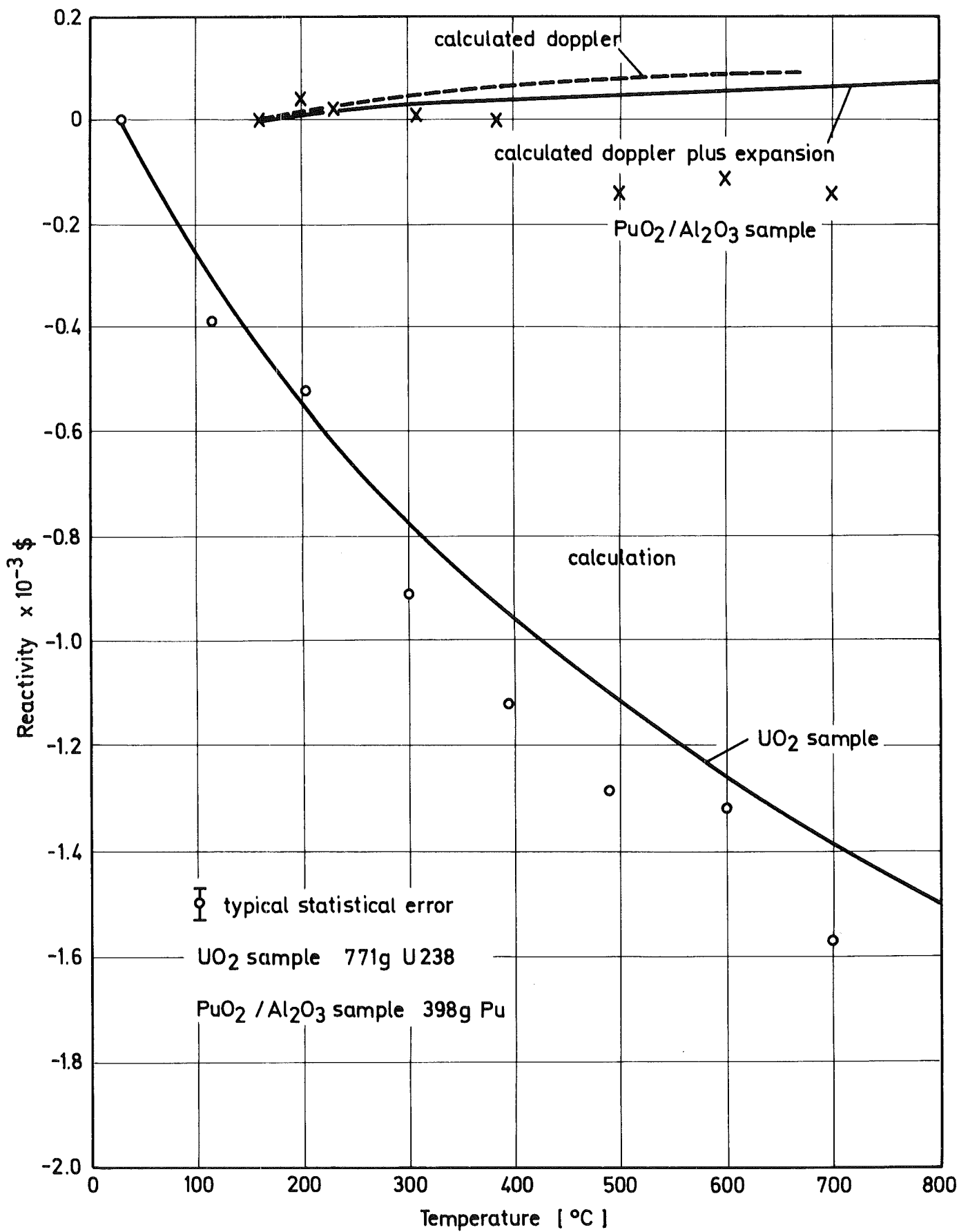


Fig. 14